

From submarine continental accretion to arc-continent orogenic evolution: The thermal record in southern Taiwan

Lucas Mesalles^{1,2,3}, Frédéric Mouthereau^{2,3,4}, Matthias Bernet⁵, Chung-Pai Chang^{1,4,6}, Andrew Tien-Shun Lin¹, Charlotte Fillon⁷, and Xavier Sengelen^{1*}

¹Institute of Geophysics, National Central University, Chungli 320, Taiwan

²Sorbonne Universités, UPMC; Univ Paris 06, UMR 7193, Institut des Sciences de la Terre Paris (ISTeP), 4 Place Jussieu, F-75005 Paris, France

³CNRS, UMR 7193, Institut des Sciences de la Terre Paris (ISTeP), 4 Place Jussieu, F-75005 Paris, France

⁴Laboratoire International Associé ADEPT, CNRS-NSC, 4 Place Jussieu, F-75005 Paris, France

⁵ISterre, Université Joseph Fourier, CNRS, 1381 Rue de la Piscine, 38041 Grenoble, France

⁶Geological Remote Sensing Laboratory, Center for Space and Remote Sensing Research, National Central University, Chungli 320, Taiwan

⁷Instituto de Ciencias de la Tierra Jaume Almera, Consejo Superior de Investigaciones Científicas (ICTJA-CSIC), Solé i Sabarís s/n, 08028 Barcelona, Spain

ABSTRACT

Constraining the timing of initial collision is critical for understanding how long-term plate convergence is accommodated at collisional plate boundaries. Reevaluation of the age of collision from orogenic thermal evolution requires distinguishing the onset of submarine continental accretion from earlier oceanic subduction and subsequent subaerial orogenic evolution. We present new thermochronological constraints from the first age-elevation relationship transect in Taiwan and zircon and apatite fission-track ages from sediments in the western foreland. Our data reveal the onset of cooling from at least 7.1 ± 1.3 Ma, at a minimum rate of $21^\circ\text{C}/\text{m.y.}$, in the submarine sedimentary wedge followed by a marked acceleration of subaerial exhumation after ca. 3.2 ± 0.6 Ma at an average rate of 1.7 km/m.y. Our data reflect the effect of margin architecture as Taiwan evolved from submarine accretion of the distal extremely thinned continental margin to crustal thickening of the proximal margin and orogenic development.

INTRODUCTION

Dating the onset of collision and subsequent stages of crustal thickening provides first-order constraints for assessing how plate convergence is accommodated to form mountain belts. The initiation of accretion of continental crust starts with the arrival of passive margins at the subduction zone and hence reflects margin architecture. Increasing evidence suggests that passive margins are constituted of ~ 200 -km-wide areas of extremely thinned continental crust rather than narrow transition zones (e.g., Reston, 2009). Orogenic development should thus include an initial stage of submarine collision before growing into subaerial mountain belts. However, such early collisional stages have seldom been described in the literature due to the difficulty of distinguishing the initial stages from the subsequent orogenic evolution.

The Taiwan orogen results from oblique plate convergence between the Philippine Sea plate and Eurasian margin (Suppe, 1981). This tectonic setting suggests the collision initiated first in the north and propagated southward, in agreement with the present observation of the transition from oceanic subduction to accretion of the hyperextended Eurasian continental crust under water ~ 150 – 200 km south of the southern tip of Taiwan (McIntosh et al., 2013; Fig. 1A).

Despite the analogy with the offshore collisional processes, the record of early continental crust involvement on land in Taiwan is poorly documented. Onset of orogenic loading-related plate flexure dated at ca. 6.5 Ma in the western Taiwan foreland (Lin et al., 2003) suggests that col-

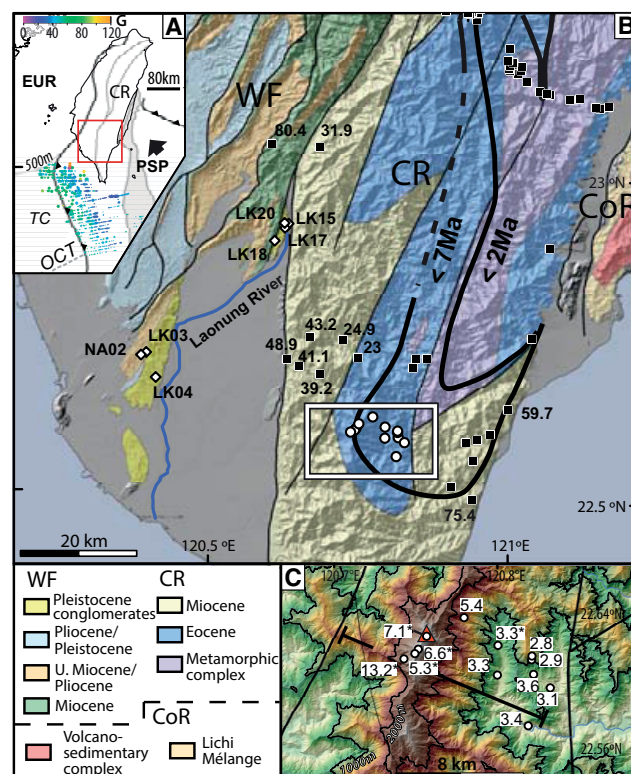


Figure 1. A: Tectonic features of the Taiwan area. EUR—Eurasian plate; PSP—Philippine Sea plate; TC—transitional crust; OCT—Ocean-continent transition; CR—Central Range. Black arrow depicts the relative velocity vector of the Philippine and Eurasian plates. Gray area indicates the Luzon volcanic arc. Gray lines onshore indicate the main structural boundaries in the Central Range, and gray line offshore indicates the 500 m bathymetric contour. Submarine shallow geothermal gradients (G, in $^\circ\text{C}/\text{km}$) from Chi and Reed (2008) are depicted in colors. **B:** Geologic map of southern Taiwan and location of samples for fission-track analyses (white circles and diamonds). Thick black lines show contour of zircon fission-track (ZFT) ages younger than 7 Ma and younger than 2 Ma (black squares) (Tsao, 1996; Liu et al., 2001; Willett et al., 2003; Lee et al., 2006). Ages are indicated for ZFT ages older than 7 Ma. WF—Western Foothills; CR—Central Range; CoR—Coastal Range; LK—Linkou and Liukuei conglomerates; NA—Nanshihulun Sandstone. **C:** ZFT ages from the age-elevation profile in Figure 2 plotted on digital elevation model with the main structural boundaries and location of cross section in Figure 2 (black line). Young peak ages are indicated with asterisks. Thin black lines depict 1000 m and 2000 m contour lines, and red triangle indicates location of the Peitawu Shan (3095 m). Geology is based on Chen et al. (2000).

*Current address: CEREGE, Aix-Marseille Université, Technopole Environnement Arbois, Méditerranée BP80, 13545 Aix en Provence, Cedex 04, France.

lision was ongoing at that time. In order to resolve the earliest stages of submarine collision, we extracted the first thermochronological age-elevation relationship in Taiwan from samples collected in the southern Central Range. The vertical profile was combined with thermochronologic analyses of Pliocene–Pleistocene detrital pro-foreland deposits, which recorded exhumation of the Central Range. Both approaches document cooling and unroofing history of the Central Range from initial accretion in the sedimentary wedge to the last stages of crustal thickening. Our results lead to a reevaluation of the timing of the first collision-related thermal perturbation affecting the rifted South China Sea (SCS) margin and subsequent orogenic growth.

GEOLOGICAL BACKGROUND AND COOLING AGE CONSTRAINTS

Deformation and accumulation of continentally derived sediments have continuously been taking place in the subduction accretionary wedge since the start of SCS subduction (ca. 15 Ma; e.g., Huang et al., 2006). Collision in Taiwan started with the arrival of Eurasian continental crust in the Manila Trench. Following the accretion of highly extended passive margin crust, the arrival of thicker continental crust onshore in northern Taiwan coincided with the closure of the forearc basin and accretion of the northernmost Luzon volcanic arc of the Philippine Sea plate (Figs. 1A and 1B). The Central Range results from the stacking of pre-rift and synrift Eocene to postrift Miocene SCS margin sediments, and its Eurasian Paleozoic–Mesozoic basement. The Western Foothills represent the western fold-and-thrust belt, composed of west-propagating thrust slices of preorogenic and synorogenic foreland sediments. The active suture between the two plates is represented by the Longitudinal Valley, along which the Lichi mélange crops out (Fig. 1B).

Apatite fission-track (AFT) ages show that the Central Range was exhumed over the past 1–2 m.y. at rates of 4–6 km/m.y. (Willett et al., 2003). Relatively recent exhumation and exposure of the metamorphic core are indicated by orogenic zircon fission-track (ZFT) cooling ages (Kirstein et al., 2010) and the first occurrence of metamorphic clasts (Dorsey, 1988) in the 2 Ma or younger deposits of the eastern retro-foredeep basin.

Liu et al. (2001) described slightly older ZFT age populations of 6–5 Ma in the northwestern and southern parts of the Central Range and interpreted them as reset ages, consistent with cooling from temperatures in excess of 260 °C. In southern Taiwan, where exhumation is considered the most recent, Willett et al. (2003) interpreted AFT ages of 5.5–1.2 Ma and ZFT ages older than 3 Ma as not related to the collisional history, despite being younger than the depositional age. By contrast, Lee et al. (2006) interpreted ZFT ages of 5.3–3.6 Ma from the same Miocene slates of the southern Central Range as fully reset, and concluded that collision dates to ca. 6 Ma, although no consistent thermochronological model was proposed to reproduce these data.

METHODS

General Approach

In this study we use fission-track dating, which provides information on the time-temperature history of rocks that have cooled in the shallow (<10 km) crust (see the GSA Data Repository¹ for analytical procedures and data treatment). Our aim is to constrain the cooling history of the orogenic wedge since (1) the first stages of collisional accretion of the thin continental crust, and (2) its later evolution as the wedge became subaerial and thicker continental crust was involved. To address this, we applied the vertically distributed samples approach (e.g., Reiners and Brandon,

2006) within the Eocene–Miocene series in the Central Range, to retrace the cooling history of this series since they were accreted in the orogenic wedge to the more recent tectonic events creating present-day topography. We sampled Pliocene–Pleistocene shallow-marine to fluvial sediments derived from the Taiwan orogen, now deformed and exposed in the southern Western Foothills fold-thrust belt. The sampled stratigraphic sections include synorogenic deposits that record a major Pleistocene tectonic-erosive event, as indicated by a coarsening upward and a major increase in sedimentation rate (Chang and Chi, 1983). These sediments provide a record of subaerial unroofing along the western side of the Central Range.

Vertical Profile Sampling and Modeling

We collected 12 samples of very low grade metamorphic Eocene and Miocene sandstone for ZFT analyses. Sampling sites range in elevation from 465 m to 3097 m and include Peitawu Shan, the highest point of southern Taiwan (Figs. 1C and 2A). The geological structure of the study area indicates that sampled sandstones are tightly folded with penetrative cleavages but with no major faults or shear zones (Figs. 1B and 2D). For samples with over-dispersed age distributions and one age population younger than the depositional age (Table DR2; see footnote 1), we used the young peak age approach, where only the youngest age peak is considered to record the last thermal event (Brandon et al., 1998; Garver et al., 2005). Young peak ages indicate resetting of the least retentive population of zircons at 180–200 °C (Garver et al., 2005) and have been widely used in Taiwan (e.g., Liu et al., 2001; Willett et al., 2003). Full annealing of all zircons requires temperatures above 260 °C (Liu et al., 2001).

To derive geothermal gradients and exhumation rates, our ZFT vertical profile results were modeled using the analytical solution of Willett and Brandon (2013) that accounts for advection of heat and the dependence of closure temperature on cooling rates. We then entered the inverted values into a forward HeFTy model (Ketchum, 2005) to independently test the fit of the data (for modeling details, see the Data Repository).

Western Foreland Samples

Seven samples were collected for AFT and ZFT analyses from Pliocene–Pleistocene wedge-top foreland basin deposits between the Western Foothills and the Central Range (Fig. 1B). The Linkou and Liukuei con-

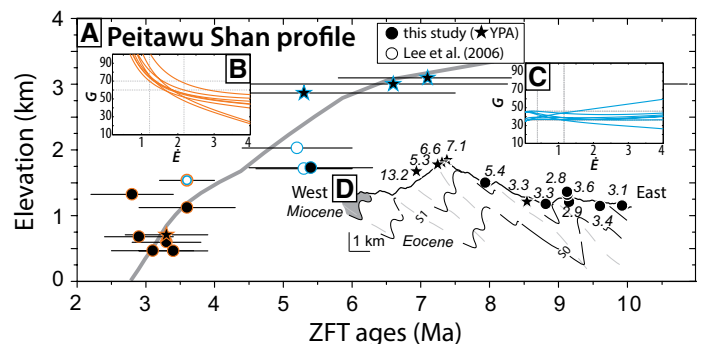


Figure 2. A: Zircon fission-track (ZFT) age-elevation profile from Peitawu Shan, Taiwan, compared with prediction of a forward thermal model (gray line). YPA—young peak age. **B, C:** Graphic representations of exhumation rate (E , in km/m.y.) versus geothermal gradients (G , in °C/km) from the inverse models results for the lower (**B**; orange, eight curves) and upper (**C**; blue, seven curves) parts of the vertical profile. Each sample is represented by one G versus E curve. Vertical and horizontal gray dashed lines indicate range of exhumation rates and geothermal gradients, respectively, recorded by the samples. One sample (in blue and orange in **A**) was used in the inversion of both the upper and lower profiles. **D:** Position of our ZFT cooling ages along an east-west geologic section (see location in Fig. 1C) based on Chen et al. (2000) and our field observations; S_0 and S_1 depict bedding and cleavage, respectively. For ZFT data, see Tables DR1 and DR2 (see footnote 1).

¹GSA Data Repository item 2014319, the thermal modelling approach, Figure DR1, and Tables DR1–DR4, is available online at www.geosociety.org/pubs/ft2014.htm, or on request from editing@geosociety.org or Documents Secretary, GSA, P.O. Box 9140, Boulder, CO 80301, USA.

glomeratic formations are the youngest studied sediments, with depositional ages younger than 2 Ma (base of nannofossil biozone NN19; Chi, 1979; Fig. 3). The conglomerates are separated by an angular unconformity from the underlying shallow-marine Nanshihlu Sandstone, dated to ca. 4 Ma (nannofossil biozone NN15; Chi, 1979; Fig. 3), representing the oldest sampled strata. We collected nonmetamorphic to very low grade metamorphic sandstone cobbles in two localities interpreted to represent lateral equivalents of the same coarsening-upward succession of a fluvial-dominated fan fed by the paleo-Laonung River catchment (Fig. 1B). The sampled sandstones represent the preorogenic Miocene to Paleogene pre-erosional cover of the Central Range.

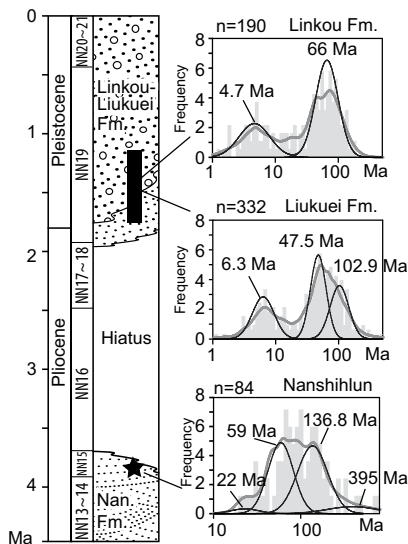


Figure 3. Depositional age and calcareous nannofossil biozones of the Linkou and Liukuei Formations and Nanshihlu Sandstone (Nan. Fm.; Taiwan) with the position of detrital zircon fission-track (ZFT) samples and corresponding ZFT grain age probability-density plot. Observed ZFT grain age probability-density plots (thick gray line) with binomial fitted peaks (thin black line) and distribution histograms are shown (an AFT grain age probability-density plot is in Fig. DR1; fission-track data are in Tables DR3 and DR4 [see footnote 1]).

RESULTS

ZFT analyses from the topographic profile have minimum ages ranging from 2.8 ± 0.6 Ma to 7.1 ± 1.3 Ma for samples to the east of the drainage divide, and display a well-defined age-elevation relationship with a break in slope at ~ 1500 m (Fig. 2A). Samples above the break in slope have minimum ZFT ages that consistently increase with elevation to 7.1 ± 1.3 Ma. Samples below the break in slope have ages that remain invariant with altitude with an average age of ca. 3.2 ± 0.6 Ma. An additional sample west of the divide has an age of 13.2 Ma (Fig. 1C) that does not correlate with the age-elevation relationship defined east of the divide, but is consistent with the spread of older (older than 20 Ma), unreset or partially reset zircons within the stratigraphically younger Miocene Lushan Formation (e.g., Lee et al., 2006) (Fig. 1B).

Inversion of the upper part of the profile (ages between 7.1 ± 1.3 Ma and 3.6 ± 0.7 Ma) provides apparent exhumation rates of 0.4–1.16 km/m.y. (0.8 km/m.y. on average) with geothermal gradients of 36–46 °C/km (Fig. 2C), equivalent to cooling rates of 21 °C/m.y. to 37 °C/m.y. For the lower part of the profile the inversion requires exhumation rates of 1.2–2.2 km/m.y. (1.7 km/m.y. on average) with geothermal gradients of 60–70 °C/km (Fig. 2B), equivalent to cooling rates of 102–119 °C/m.y.

ZFT dating of ~ 600 detrital zircon grains from the western foreland shows ages older than the depositional age, indicating no significant post-depositional resetting. The 2 Ma conglomerates display slightly different age components (Fig. 3; Table DR3); the youngest populations, 4.7 ± 0.7 Ma and 6.3 ± 0.8 Ma, are those of the Linkou and Liukuei conglomerates, respectively. These ages are the first record of mountain building in the western foreland and are similar to the ZFT ages from the upper part of the vertical profile. Older populations of 47.5 ± 6.2 and 66 ± 8.2 Ma represent pre-orogenic zircons. ZFT analyses in the 4 Ma Nanshihlu Sandstone

yielded the same pre-orogenic age population of 59 ± 8.3 Ma and a distinctive older age peak of 136.8 ± 21.6 Ma. AFT dating of ~ 70 apatites in the Linkou and Liukuei samples confirms the appearance of young grains in the 2 Ma deposits with a young peak population of 4.7 ± 0.5 Ma (Fig. DR1; Table DR4).

DISCUSSION AND CONCLUSIONS

Our data document an initial phase of cooling from at least ca. 7.1 Ma to ca. 3.2 Ma, as recorded in the vertical profile (Fig. 2A) and in the sediments younger than 2 Ma (Fig. 3), followed by a drastic increase in average exhumation rates ca. 3.2 Ma (Fig. 2B). Older ZFT populations (older than 20 Ma) in both sets of samples (Tables DR2 and DR3) record the predepositional Jurassic–Cretaceous tectono-magmatic events in the Chinese margin source areas (e.g., Kirshtein et al., 2010). Early orogenic zircon populations start appearing in the southern pro-foreland basin from ca. 2 Ma, similar to the post-2 Ma retro-foredeep sediments yielding distinctive zircon populations from 7.9 to 4.9 Ma (Kirshtein et al., 2010).

Conversely to the retro-foredeep record, our 2 Ma western foreland sediments do not contain ca. 3 Ma ZFT ages. These observations suggest that the ca. 3.2 Ma phase exhumed principally the retrowedge, whereas the early cooling phase from at least 7.1 Ma onward appears to have affected the entire Central Range equally. This late phase is possibly responsible for the rapid exhumation of the metamorphic core.

An early cooling phase contrasts with interpretations that suggest that ZFT ages older than 3 Ma are not related to the collision evolution (Fuller et al., 2006; Willett et al., 2003). Because the Taiwan wedge emerged ca. 5 Ma (Teng, 1990), it may seem difficult to conceive collision-related cooling in a submarine accretionary prism, as we usually associate cooling with subaerial exhumation of rocks. Processes other than erosion may explain such apparent contradiction, namely, underwater extensional unroofing and/or cooling from below by the lower underthrusting plate characteristic of subduction zones.

The latter appears to be the most likely and dominant process, given the analogy with the ongoing continental underthrusting observed offshore southern Taiwan (McIntosh et al., 2013). The present-day geothermal gradients offshore Taiwan decrease from the undeformed distal margin and lower slope of the accretionary wedge (70–80 °C/km) to the upper slope of the accretionary wedge (30–40 °C/km) (Fig. 1A; Chi and Reed, 2008). The latter values are remarkably consistent with our inverted gradients of 36–46 °C/km for the early stage of cooling.

Whether 7.1 ± 1.3 Ma marks the onset, or is only the preserved relic, of a longer cooling phase remains arguable; nonetheless, our data are consistent with an initiation of cooling at that time. Our topmost samples have undergone conditions between 58 °C and 74 °C colder than the samples below the break in slope. This implies that while the lower samples were at temperatures in excess of 260 °C, the topmost one was between 186 °C and 202 °C, suggesting that low-retention zircons in this sample recorded the very first effects of underthrusting-related cooling and date the onset at 7.1 ± 1.3 Ma.

Figure 2 shows the fit of predicted ZFT age-altitude relationship using inverted values on timing and geothermal gradients with the age-elevation data. We infer that after the break-up stage at 30 Ma, postrift sediments of the Chinese margin recorded a period of isothermal holding, followed by the onset of cooling by 7.1 ± 1.3 Ma and increasing of cooling rates at 3.2 ± 0.6 Ma. We conclude that the studied sediments recorded the earliest stage of continental accretion on top of the underthrust margin of the SCS (Fig. 4).

Accelerated exhumation documented at ca. 3.2 ± 0.6 Ma occurred coevally with formation of a ubiquitous angular unconformity (Fig. 3) and increased tectonic subsidence in the foreland (e.g., Lin et al., 2003). This followed the accretion of the Luzon arc to the orogen, as recorded by the age of the Lichi ophiolitic mélange formation, 3.7–3.5 Ma (Chang et al., 2009). Fast heat advection due to increasing erosion is consistent

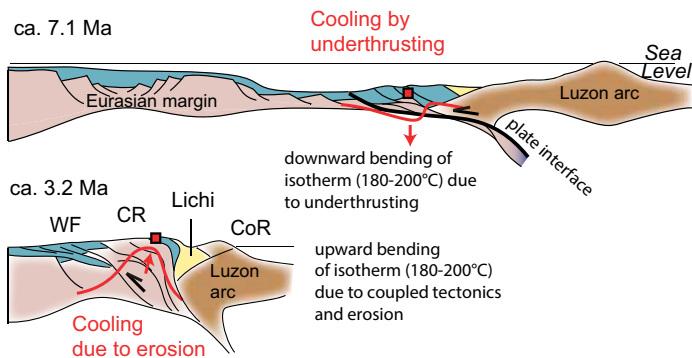


Figure 4. Tectonic evolution of the Taiwan arc-continent collision that integrates our results on initial cooling ca. 7.1 Ma related to inversion of the distal Eurasian margin and subsequent accelerated exhumation after ca. 3.2 Ma associated with Luzon arc collision. Red line presents schematic isotherms deflected downward during underthrusting of the distal margin, then upward as the proximal margin thickened and erosion rate increased. Square is the approximate location of the age-elevation profile. WF—Western Foothills; CR—Central Range; Lichi—Lichi ophiolitic mélange CoR—Coastal Range.

with higher gradients of ~ 60 °C/km reconstructed for this period. It agrees remarkably well with currently observed gradients in the Central Range (Chi and Reed, 2008).

Our results show that the Taiwan collision had started by 7.1 ± 1.3 Ma, with the accretion of the distal margin of the SCS. A stepwise increase in exhumation starting ca. 3.2 ± 0.6 Ma recorded the transition toward shortening of a thicker margin section, which eventually led to major topographic growth and erosion. Our timing for initial collision-related cooling is in agreement with the generally accepted age of late Cenozoic metamorphism as defined by a mineral neof ormation age of 8–7 Ma in northern Taiwan plutonic bodies (Lo and Onstott, 1995). This implies synchronous initial collision along the island, and not the southward-propagation model of the collision as inferred by a straight continental margin.

ACKNOWLEDGMENTS

We thank S. Willett for his advice during inverse modeling, and E. Hardwick, F. Senebier, and F. Coeur for help during sample preparation. We also thank T.-F. Yui for providing access to the sample processing facilities at the Institute of Earth Sciences, Academia Sinica, Taiwan, and S. Giletycz, O. Giletycz, and H. Giletycz for their assistance in the field and as hosts. Mesalles was supported by LIA ADEPT (Associated International Laboratory Active Deformation and Environment Programme for Taiwan) between the National Science Council (Taiwan) and the French CNRS (Centre National de la Recherche Scientifique), and Université Pierre et Marie Curie. Mouthereau benefited from a Partenariats Hubert Curien Program Orchid grant provided by the French Ministry of Foreign Affairs. Editor J. Spotila, J. Buscher, J.-D. Champagnac, and anonymous reviewers contributed to the improvement of the manuscript.

REFERENCES CITED

Brandon, M.T., Roden-Tice, M.K., and Garver, J.I., 1998, Late Cenozoic exhumation of the Cascadia accretionary wedge in the Olympic Mountains, north-west Washington State: *Geological Society of America Bulletin*, v. 110, p. 985–1009, doi:10.1130/0016-7606(1998)110<0985:LCEOTC>2.3.CO;2.

Chang, C.-P., Angelier, J., and Huang, C.-Y., 2009, Evolution of subductions indicated by mélanges in Taiwan, in Lallemand S., and Funicello F., eds., *Subduction zone geodynamics*: Berlin Heidelberg, Springer-Verlag, p. 207–225, doi:10.1007/978-3-540-87974-9.

Chang, S.S.L., and Chi, W.-R., 1983, Neogene nannoplankton biostratigraphy in Taiwan and the tectonic implications: *Petroleum Geology of Taiwan*, v. 19, p. 93–147.

Chen, C.-H., Ho, H.-C., Shea, K.-S., Lo, W., Lin, W.-H., Chang, H.-C., Huang, C.-W., Chen, C.-H., Yang, C.-N., and Lee, Y.-H., 2000, Geological map of

Taiwan: Taiwan Central Geological Survey Ministry of Economic Affairs, scale 1:500,000.

Chi, W.-C., and Reed, D.L., 2008, Evolution of shallow, crustal thermal structure from subduction to collision: An example from Taiwan: *Geological Society of America Bulletin*, v. 120, p. 679–690, doi:10.1130/B26210.1.

Chi, W.-R., 1979, A biostratigraphic study of the late Neogene sediments in the Kaoshiung area based on calcareous nanofossils: *Geological Society of China Proceedings*, v. 22, p. 121–144.

Dorsey, R.J., 1988, Provenance evolution and unroofing history of a modern arc-continent collision: Evidence from petrography of Plio-Pleistocene sandstones, eastern Taiwan: *Journal of Sedimentary Petrology*, v. 58, p. 208–218.

Fuller, C., Willett, S.D., Fischer, D., and Lu, C.-Y., 2006, A thermomechanical wedge model of Taiwan constrained by fission-track thermochronometry: *Tectonophysics*, v. 425, p. 1–24, doi:10.1016/j.tecto.2006.05.018.

Garver, J.I., Reiners, P.W., Walker, L.J., Ramage, J.M., and Perry, S.E., 2005, Implications for timing of Andean uplift from thermal resetting of radiation-damaged zircon in the Cordillera Huayhuash, northern Peru: *Journal of Geology*, v. 113, p. 117–138, doi:10.1086/427664.

Huang, C.-Y., Yuan, P.B., and Tsao, S.-J., 2006, Temporal and spatial records of active arc-continent collision in Taiwan: A synthesis: *Geological Society of America Bulletin*, v. 118, p. 274–288, doi:10.1130/B25527.1.

Ketchum, R.A., 2005, Forward and inverse modeling of low-temperature thermochronometry data: *Reviews in Mineralogy and Geochemistry*, v. 58, p. 275–314, doi:10.2138/rmg.2005.58.11.

Kirstein, L.A., Fellin, M.G., Willett, S., Carter, A., Chen, Y.-G., Garver, J.I., and Lee, D.C., 2010, Pliocene onset of rapid exhumation in Taiwan during arc-continent collision: New insights from detrital thermochronometry: *Basin Research*, v. 22, p. 270–285, doi:10.1111/j.1365-2117.2009.00426.x.

Lee, Y.-H., Chen, C.-C., Liu, T.-K., Ho, H.-C., Lu, H.-Y., and Lo, W., 2006, Mountain building mechanisms in the Southern Central Range of the Taiwan Orogenic Belt—From accretionary wedge deformation to arc-continent collision: *Earth and Planetary Science Letters*, v. 252, p. 413–422, doi:10.1016/j.epsl.2006.09.047.

Lin, A.T., Watts, A.B., and Hesselbo, S.P., 2003, Cenozoic stratigraphy and subsidence history of the South China Sea margin in the Taiwan region: *Basin Research*, v. 15, p. 453–478, doi:10.1046/j.1365-2117.2003.00215.x.

Liu, T.-K., Hsieh, S., Chen, Y.-G., and Chen, W.-S., 2001, Thermo-kinematic evolution of the Taiwan oblique-collision mountain belt as revealed by zircon fission track dating: *Earth and Planetary Science Letters*, v. 186, p. 45–56, doi:10.1016/S0012-821X(01)00232-1.

Lo, C.-H., and Onstott, T.C., 1995, Rejuvenation of K/Ar systems for minerals in the Taiwan Mountain Belt: *Earth and Planetary Science Letters*, v. 131, p. 71–98, doi:10.1016/0012-821X(95)00011-Z.

McIntosh, K., van Avendonk, H., Lavier, L., Lester, W.R., Eakin, D., Wu, F., Liu, C.-S., and Lee, C.-S., 2013, Inversion of a hyper-extended rifted margin in the southern Central Range of Taiwan: *Geology*, v. 41, p. 871–874, doi:10.1130/G34402.1.

Reiners, P.W., and Brandon, M.T., 2006, Using thermochronology to understand orogenic erosion: *Annual Review of Earth and Planetary Sciences*, v. 34, p. 419–466, doi:10.1146/annurev.earth.34.031405.125202.

Reston, T.J., 2009, The structure, evolution and symmetry of the magma-poor rifted margins of the North and Central Atlantic: A synthesis: *Tectonophysics*, v. 468, p. 6–27, doi:10.1016/j.tecto.2008.09.002.

Suppe, J., 1981, Mechanics of mountain building and metamorphism in Taiwan: *Geological Society of China Memoirs*, v. 4, p. 67–89.

Teng, L.-S., 1990, Geotectonic evolution of late Cenozoic arc-continent in Taiwan: *Tectonophysics*, v. 183, p. 57–76, doi:10.1016/0040-1951(90)90188-E.

Tsao, S.-J., 1996, The geological significance of illite crystallinity, zircon fission-track ages and K-Ar ages of metasedimentary rocks of the Central Range [Ph.D. thesis]: Taipei, Taiwan, National Taiwan University, p. 272.

Willett, S.D., and Brandon, M.T., 2013, Some analytical methods for converting thermochronometric age to erosion rate: *Geochemistry Geophysics Geosystems*, v. 14, p. 209–222, doi:10.1029/2012GC004279.

Willett, S.D., Fischer, D., Fuller, C., Yeh, E.-C., and Lu, C.-Y., 2003, Erosion rates and orogenic-wedge kinematics in Taiwan inferred from fission-track thermochronometry: *Geology*, v. 31, p. 945–948, doi:10.1130/G19702.1.

Manuscript received 9 May 2014

Revised manuscript received 24 July 2014

Manuscript accepted 30 July 2014

Printed in USA